Tellus (1981), *33*, 188–200

Stability properties of an arbitrarily oriented mean flow

By RICHARD GROTJAHN, *National Center for Atmospheric Research*,[1] *Boulder, CO 80307, U.S.A.*

(Manuscript received June 6; in final form August 19, 1980)

ABSTRACT

The linear properties of eddies growing in a mean flow that is oriented in any horizontal direction are analyzed. The mean flow only varies with height. The growth rate, phase speed and structure of the waves change dramatically with different orientations of the mean flow and the waves. These properties are related to the vertical profile of the mean total interior potential vorticity gradient, $\bar{Q}$. $\bar{Q}$ is largest for those orientations where the Coriolis terms are most positive; it is smallest when those terms are most negative. When $\bar{Q}$ is maximized; the growth rates are largest, the propagation speed is least, the upper level eddy amplitude is enhanced and the sharpest vertical tilts of the trough and ridge axes occur at lower levels. The opposite properties result when $\bar{Q}$ is minimized. Limiting the horizontal extent of the wave (by using side-wall boundaries) causes cross-flow asymmetry in the wave structure and induces horizontal tilts to the wave axes.

1. Introduction

Geophysical fluid flows are characterized by complicated spatial structure. The local variations in the flow might be categorized according to mean direction, curvature and turning as well as straight horizontal and vertical shear. It would be useful to be able to examine the stability properties of small regions of a complex flow, instead of restricting analysis to larger scale, highly idealized mean flows. Such a "local stability analysis" would not only tell us about the nature and evolution of waves imbedded in a more typical flow, but it could also describe variations in the predictability of that flow. In baroclinic and barotropic instability studies it has been convenient to restrict the analysis to mean flows without curvature or turning. In addition, it is common practice to orient the prescribed flow in the zonal direction. These constraints result in a considerable simplification of the mathematics. However, actual geophysical flows are rarely confined to the zonal direction. This is true in the atmosphere and especially in the ocean, where the basin shape exerts an important influence. This study removes the restraint upon the orientation of a prescribed flow which only varies with height. In this narrow sense, this work constitutes a further step toward a local stability analysis of complex geophysical flows.

Not all previous studies were restricted to zonal flows with zonally propagating eddies. Miles (1964) allowed the waves in his baroclinic instability study to propagate in any horizontal direction, but he required his mean flow to be zonal. Robinson and McWilliams (1974) used a two-layer model that allowed mean currents of any compass direction in their study of mesoscale oceanic eddies. Both works found that the wave propagating parallel to the mean flow grew the fastest. This result is not necessarily general. The following experiments indicate that there can be wavelengths at special orientations of the mean flow where the waves propagating at an angle to that flow amplify fastest. Brode and Mak (1978) examined the stability of flows with turning but the important variation of the Coriolis parameter was neglected in their model. Killworth (1979) examined the propagation of neutral Rossby waves in mean flows of various orientations and shear. The stability of a plane wave propagating in any direction to a mean

[1] The National Center for Atmospheric Research is sponsored by the National Science Foundation.

0040-2826/81/020188-13$02.50/0

flow of arbitrary orientation was briefly discussed by Pedlosky (1979) using a two-layer model. He showed that, for *nonzonal* mean flows, there may be no minimum shear required for instability despite the linearly variable Coriolis parameter. He also found that the most unstable wave does not necessarily propagate parallel to the mean flow, especially when the mean shear is weak. In this report, analogous plane wave solutions are examined in more detail and without the restriction of two layers. Also, some wave-like solutions of finite horizontal extent are considered here.

Eigenvalue problems which include a wave in the basic state (and hence, curvature) were examined by Frederiksen (1979, and its references) and Niehaus (1980). It is not clear what role, if any, is played by curvature, since those authors found preferred regions of growth could be related to regions of greatest vertical shear.

This article examines the linear stability properties of waves growing in a prescribed mean flow that can be oriented in any compass direction. The only anisotropy in the mathematical model arises from the linearly variable Coriolis parameter. The growth rate, phase speed and structure of the wave vary significantly with its direction of propagation and the direction of the mean flow. These variations can be partly traced to the mean flow potential vorticity gradient.

2. Model description

The mathematical model used in this study is similar to the model developed in Grotjahn (1979, 1980). Modifications have been introduced in order to handle the variable orientation of the mean flow.

The fluid motion satisfies the quasi-geostrophic potential vorticity equation expressed on a mid-latitude β-plane. Periodic boundary conditions are used in the along-mean-flow (x) direction. (The Appendix contains a list of symbols.) The vertical velocity vanishes at the top ($z = 5$) and bottom ($z = 0$) surfaces. The z boundary conditions are formulated from the adiabatic equation. An upper rigid lid is reasonable for this type of study because of its high placement (50 km). Both periodic and Dirichlet cross-mean-flow (y) boundary conditions are investigated. Periodic boundary conditions in y made the equations separable while allowing plane wave solutions. Dirichlet boundary conditions in y left nonseparable equations with wave-like solutions of finite horizontal width.

The prescribed fields identified as the Narrow tropopause case and lowest-order mean flow in Grotjahn (1980) are used here. The equations are linearized about this mean flow which only varies with height. The basic current U vanishes at $z = 0$ and reaches a maximum near the tropopause (Fig. 1). The stratosphere and troposphere are modelled by vertical variations in the static stability and in the log derivative of density.

The vorticity equation can be written

$$q_t + Uq_x + U\beta\cos\gamma + \phi_x\bar{q}_y = \phi_y\beta\cos\gamma \qquad (1)$$

where nonlinear terms are neglected, subscripts denote differentiation,

$$q = \varepsilon\phi_{zz} + (\Omega\varepsilon + \varepsilon_z)\phi_z + \phi_{yy} + \phi_{xx}$$

$$\bar{q}_y = -\varepsilon U_{zz} - (\Omega\varepsilon + \varepsilon_z)U_z + \beta\sin\gamma$$

U is the prescribed mean flow and γ is the orientation angle of the mean flow, measured clockwise from the northward direction (Fig. 2). Coefficients ε, Ω and U are functions of z, β is a constant.

In order to handle the nonperturbation ($U\beta\cos\gamma$) term, eq. (1) is partitioned into mean flow and nonzero wavenumber equations:

$$(\varepsilon\phi_{zz} + (\Omega\varepsilon + \varepsilon_z)\phi_z + \phi_{yy})_t = (\phi_y - U)\beta\cos\gamma \qquad (2a)$$

and

$$q_t + Uq_x + \phi_x\bar{q}_y = \phi_y\beta\cos\gamma \qquad (3a)$$

with

$$\phi_{zt} + U\phi_{zx} - U_z\phi_y = 0 \quad \text{at} \quad z = 0 \text{ and } 5 \qquad (4)$$

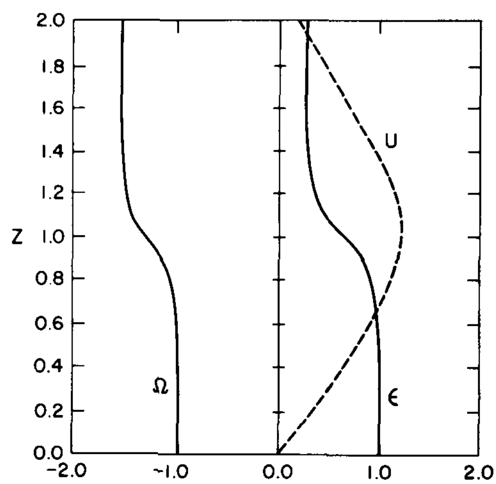

Fig. 1. Vertical profiles of ε, Ω and U for the Narrow tropopause case.

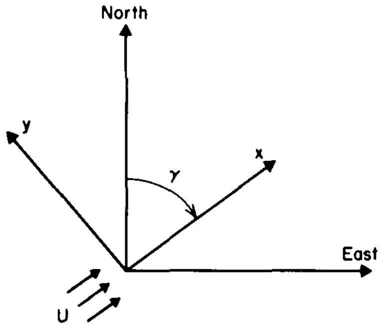

Fig. 2. Schematic illustration of the coordinate axes x and y for orientation angle γ. The mean flow U is directed as shown.

Assume a wave-like dependence in y as well as for x and t:

$$\phi = \phi(z) \exp(i(kx - \omega t + my))$$

and that $m = rk$ where r is a finite constant. For $r > 0$, the plane waves move left across the flow as one looks downstream; for $r < 0$ the waves are right-moving. Then the mean flow equation becomes (since $k = 0 = m$)

$$(\varepsilon\phi_{zz} + (\Omega\varepsilon + \varepsilon_z)\phi_z)_t = -U\beta \cos\gamma \tag{2b}$$

and the nonzero wavenumber equation becomes

$$(-i\omega + ikU)(\varepsilon\phi_{zz} + (\Omega\varepsilon + \varepsilon_z)\phi_z - \alpha^2\phi) + ik\phi\bar{q}_y = im\phi\beta\cos\gamma \tag{3b}$$

with $\alpha^2 = m^2 + k^2$ and

$$(-i\omega + ikU)\phi_z - ikU_z\phi = 0 \quad \text{at} \quad z = 0 \text{ and } 5$$

If (2a) is solved as is, it may have oscillatory or steady-state solutions depending upon the boundary conditions. If the t dependence is left unprescribed, (2b) may have linearly growing solutions. Typically, the problem is not derived in quite this way. Instead, an external forcing is introduced to balance the infinite source of planetary vorticity advected by the $U\beta\cos\gamma$ term (e.g., Pedlosky, 1979). However, both approaches accomplish the same result; namely this forcing is removed from the perturbation stability analysis. Both approaches derive equivalent versions of the perturbation equations (3). We are not interested in the solutions of (2). Instead, this article focusses upon solutions of the eigenvalue problem posed by (3). The eigenvalue is the phase frequency ω and the eigenfunction is the quasi-geostrophic pressure ϕ.

The separable eigenvalue problem (3b) yields plane wave solutions. These solutions are obtained by finite differencing (3b) and utilizing a highly accurate matrix eigenvalue routine. Several different values of r were considered. For $m = 0$, the plane waves propagate in the direction of the basic flow. For $m = k$, the waves propagate at a 45° angle to the mean flow.

The nonseparable eigenvalue problem (3a) is used for a channel domain oriented in the basic current direction. The boundary conditions $\phi = 0$ are imposed along the y = constant side-walls. The wave-like solutions have finite horizontal width and propagate in the x direction. Neither an eigenvalue nor a direct Poisson solving routine that could accurately handle a nonseparable two-dimensional equation with complex coefficients was available. Instead, (3a) was solved using perturbation methods. The mathematical procedure is presented in McIntyre (1970) along with some discussion of its validity. The numerical formulation of this approach is described in Grotjahn (1979). To properly solve (3a), this method requires the right-hand side term to be formally small. This is accomplished by restricting the range of γ. At lowest order in the small parameter expansion this term is neglected. At higher orders this term is a known forcing function. Both ω and ϕ are expanded in powers of the small parameter. The lowest-order ω and ϕ are the eigensolutions of the homogeneous equations. At each higher order, the forcing function must satisfy an orthogonality condition that specifies a corresponding term in the ω series. At lowest order ϕ is symmetric in y, so the forcing function at second order is antisymmetric. The orthogonality condition involves a symmetric integral of the forcing function, making the second-order term in the phase frequency series zero. Ergo, the phase frequencies of channel solutions are equivalent, to second order, with those of the $m = 0$ plane waves. However, the structures of the channel and plane wave solutions are significantly different.

3. Plane wave solutions

In this section the stability, motion and structure of the plane wave solutions are analyzed. The stability of similar plane wave solutions for a two-layer model are briefly described by Pedlosky (1979). Complex phase frequency spectra are plotted versus α and γ, where α is the absolute wavenumber and γ is the angle of mean-flow orientation. At $\gamma = 90$ the mean flow is from the west; at $\gamma = 180$ it is from the north. The Rossby radius of deformation (~ 1100 km) is used for the horizontal length scale. The dimensional wavelength for $\alpha = 2.0$ is about 4500 km. The solutions for $1.5 \leq \alpha \leq 2.5$ will be referred to as the intermediate waves and are emphasized in this report. The solutions for smaller or larger α are termed the long and short waves respectively. It will be useful to define a total potential vorticity gradient

$$\bar{Q} = \bar{q}_y - r\beta \cos \gamma$$

which sums both components of the basic state potential vorticity gradient. The characteristic structures of the intermediate and short waves are represented by the $\alpha = 2.0$ and $\alpha = 3.0$ solutions. The desired solutions were distinguished from the unwanted continuum or critical layer modes by selecting the solution with the largest growth rate. This procedure worked well for the intermediate and most short waves, but it was unsatisfactory for the nearly neutral long waves.

Growth rate spectra for three definitions of m are presented in Fig. 3. It is immediately clear that the stability of a wave varies a great deal depending upon its orientation to the mean flow and the planetary vorticity gradient. The most unstable wave occurs at an intermediate wavelength which also varies with γ. For flows with an easterly component, the plane waves have much smaller growth rates than for flows with a westerly component. Between these two extremes are two angles at which large growth rates extend into the long wavelengths. These intrusions of instability are centered at the values of γ satisfying $r = \tan(\gamma)$, where the two terms containing β in (3b) cancel. Whether they are positive or negative, the presence of β terms always reduces the long waves instability. These intrusions may correspond to the tongues of longer wave instability found by Robinson and McWilliams (1974, see their Fig. 9). They also found a sharp short-wave, instability cut-off which may be due to their limitation of two vertical layers.

For most values of α and γ, the fastest amplifying waves are those that propagate parallel to the mean flow. That is, those for $m = 0$. A similar pattern of growth rate variation occurs for each choice of r. And, different r values translate this characteristic pattern along the γ axis. As r increases, the overall magnitude of the growth rates become less. But, because the pattern has large variation with γ, there are small bands of wavelengths at certain angles for which the most unstable waves propagate at an angle to the mean flow. These properties are seen in Fig. 3. For example, some of the $m = k$ long waves at $\gamma = 225$ and 45 grow faster than the corresponding $m = 0$ waves. From the symmetry of (3a), a similar statement can be made for $m = -k$ and $\gamma =$ 315 and 135.

Phase speed spectra for three choices of r are displayed in Fig. 4. The chaotic regions occur where the selection procedure for obtaining the

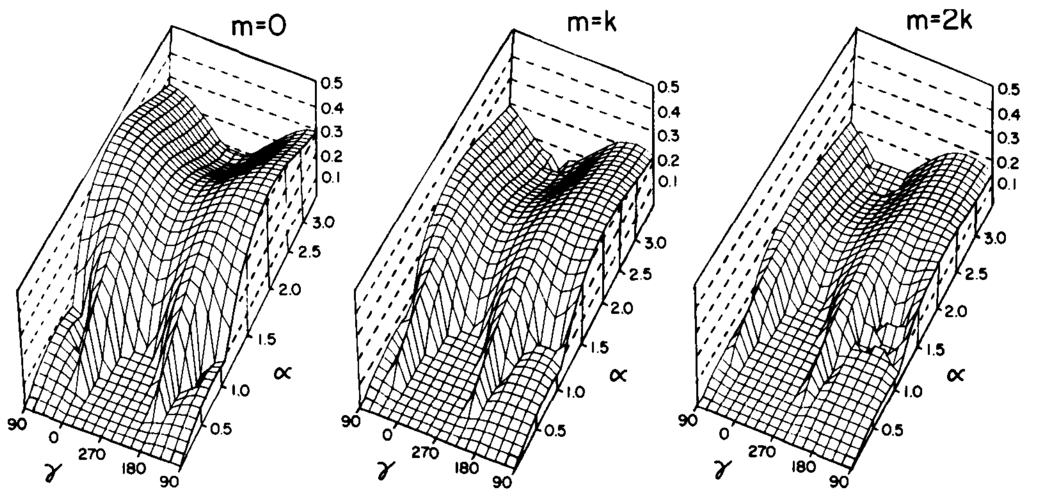

Fig. 3. Growth rate spectra versus α and γ for the Narrow tropopause case where $r = 0$ (left plot), $r = 1$ (middle plot) and $r = 2$ (right plot).

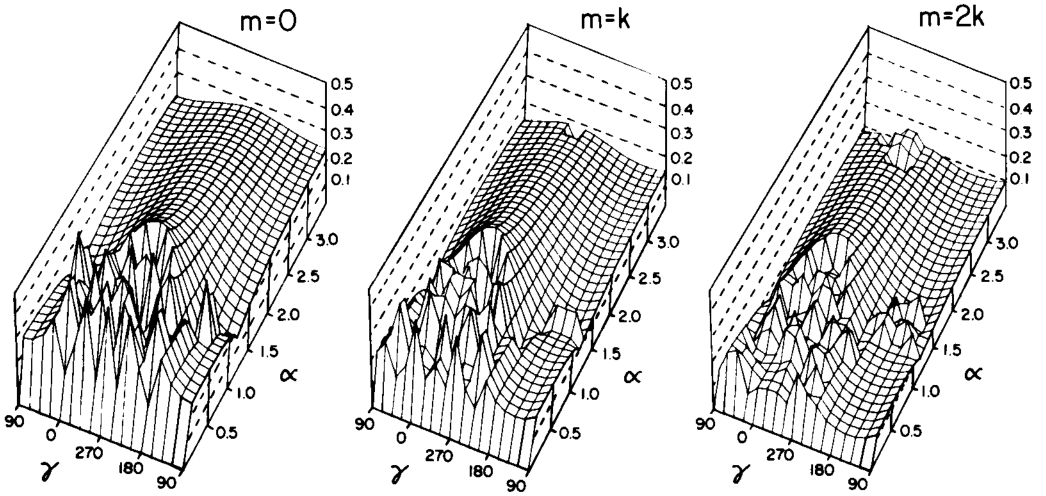

Fig. 4. Phase speed spectra for the plane waves depicted in Fig. 3.

desired eigenvalue is unsuitable. The solutions in these regions are ignored. The phase speed also changes significantly with γ. In general, the faster moving waves are those waves imbedded in easterly-type flows. For an intermediate or short wavenumber α, waves propagating fastest grow the slowest and vice versa. The intermediate waves for $r = \tan(\gamma)$ are nearly nondispersive.

If one considers an incompressible fluid and a basic current that linearly varies with height, then $\bar{Q}$ is uniform and comprises solely the two β terms. When the rigid lid is placed at $z = 1$, the problem reduces to that examined by Eady (1949) when $r = \tan(\gamma)$. At other angles the problem becomes analogous to that studied by Green (1960). Flows from the south and east induce upper trapped short waves; north and west induce lower. In this Eady–Green problem, the phase speed also reaches a maximum at a single value of γ and a minimum for basic flow in the opposite direction (Fig. 5). However, the pattern of the growth rate spectra is somewhat different for this problem. These growth rate and phase speed results can be better understood after examining the amplitude profiles.

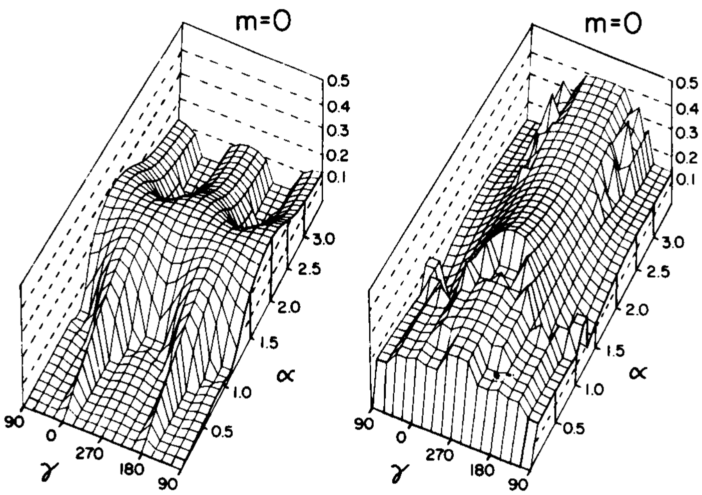

Fig. 5. Growth rate (left) and phase speed (right) spectra versus α and γ for the $m = 0$, Eady–Green waves. $\Omega = 0$, $\varepsilon = 1$, $U = z$, and the upper rigid lid is at $z = 1$.

The vertical structure of the $m = 0$ intermediate waves for six different orientation angles γ is depicted in Fig. 6. Figs. 7 and 8 show the corresponding profiles for $m = k$ and $m = 2k$. The structure is presented in terms of the wave amplitude and phase. In an eigenvector problem the amplitude and phase are specified up to an arbitrary complex constant. This constant was chosen so that the amplitude equals one and the phase is zero at the bottom.

The amplitude is characterized by two relative maxima; one near $z = 0.8$ and the other at the bottom surface. The lower maximum is fixed by the normalization, while the upper maximum changes

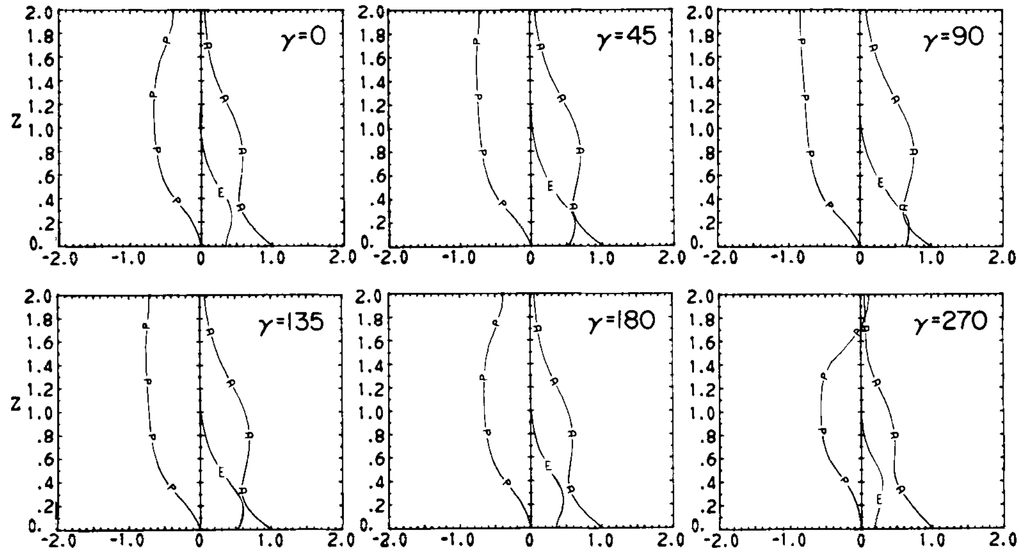

Fig. 6. Vertical profiles of amplitude (A) and one-half phase angle (P) of ϕ for the $m = 0$, intermediate ($\alpha = 2.0$), plane wave at six orientation angles. (The phase angle is divided in half.) Vertical profiles of the mean to eddy available potential energy conversion (E) are also shown.

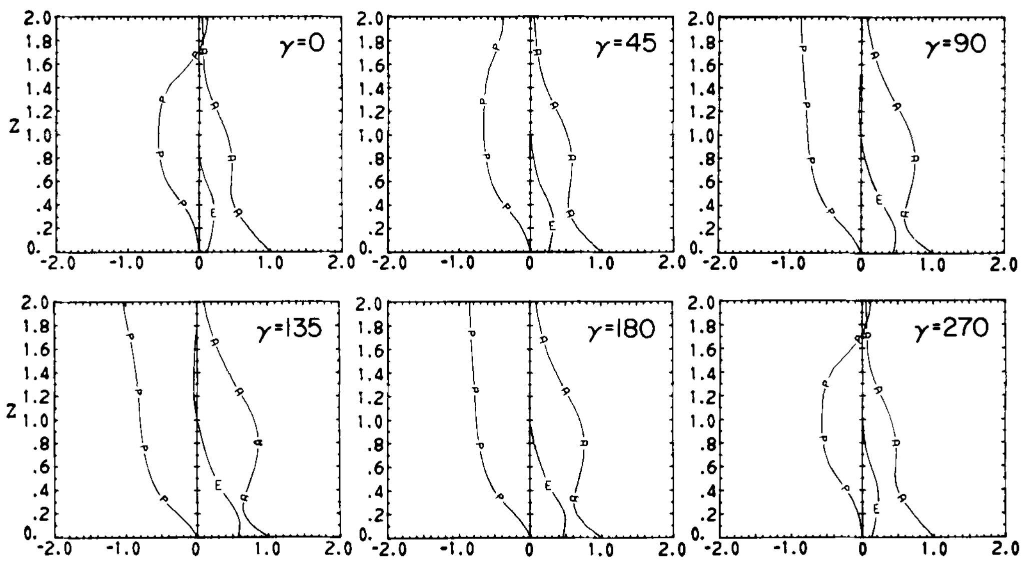

Fig. 7. Same as Fig. 6 except $m = k$.

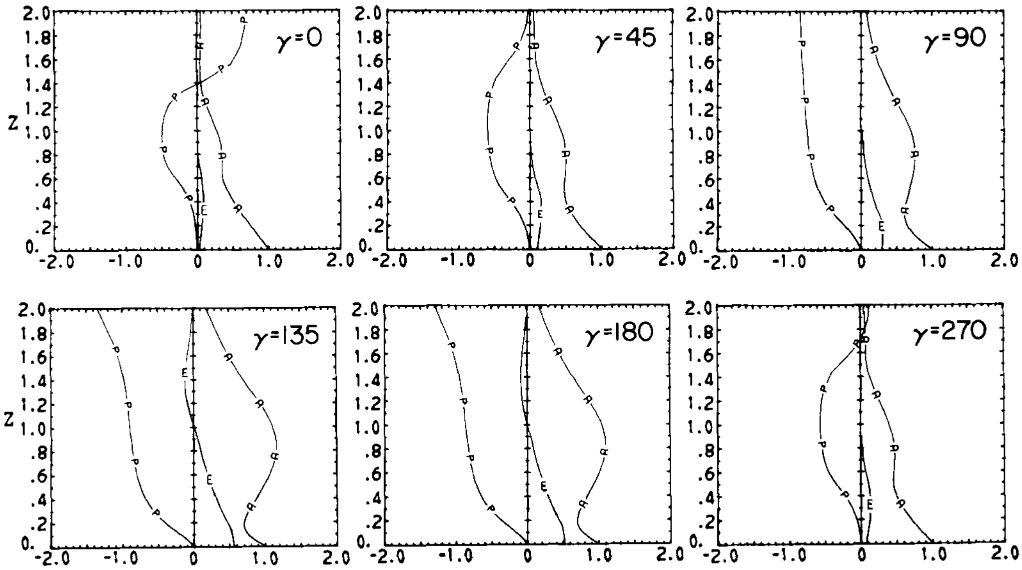

Fig. 8. Same as Fig. 6 except $m = 2k$.

for different γ. The upper maximum appears to be associated with the maximum value of the total interior potential vorticity gradient, $\bar{Q}$ shown in Fig. 9. For $m = 0$, the profiles are symmetric about the east and west directions. For example, the profiles for $\gamma = 45$ and 135 are the same. For $m = k$, the profiles are symmetric about the $\gamma = 135$ and 315 directions, making the profiles for $\gamma = 90$ and 180 identical, for example. The symmetry angles are those γ which satisfy $r = \tan(\gamma + 90)$ and are where the β terms in $\bar{Q}$ are largest or smallest. For the waves propagating along the flow ($m = 0$), the upper level amplitude is least for easterly flow. The upper level maximum is largest for westerly flow.

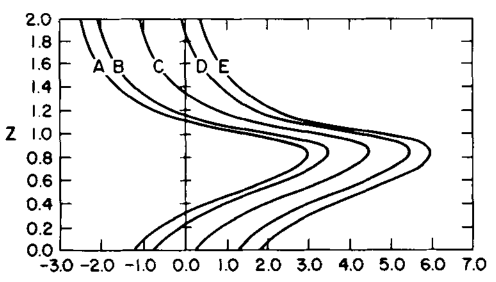

Fig. 9. Vertical profiles of Q for the Narrow tropopause for several values of γ and r. In (A) $m = k$ and $\gamma = 315$; in (B) $m = k$ or $m = 0$ and $\gamma = 270$; in (C) $m = k$ and $\gamma =$ 45 or 225, or $m = 0$ and $\gamma = 0$ or 180; in (D) $m = k$ or $m = 0$ and $\gamma = 90$; in (E) $m = k$ and $\gamma = 135$.

Hence, the upper level maximum is largest where the β terms in $\bar{Q}$ are largest and conversely. For the waves moving at an angle to the mean flow, the upper level amplitude changes by a greater amount over the range of γ. The magnitude of this amplitude variation increases with r as does the range of the β terms in $\bar{Q}$. The height of the low-level relative minimum varies with γ as well. The height is lowest for westerly flow and highest for easterly flow. The range of the heights as γ is varied increases with r also. This range appears to be tied not only to $\bar{Q}$, but also to the phase speed of the wave. That is, the height of the relative minimum is related to the steering level. Clearly the amplitude structure of the wave is strongly influenced by the distribution and magnitude of $\bar{Q}$.

In the Eady–Green problem there are relative maxima in the amplitude at the top and bottom surfaces. $\bar{Q}$ is uniform with height, being merely the sum of the two β terms. The upper surface amplitude changes in analogous fashion to the Narrow tropopause case. It is largest when $\bar{Q}$ is largest and vice versa. The height of the minimum amplitude also shifts in accordance with $\bar{Q}$ and the steering level.

The phase angle is measured positive down the direction of wave propagation. Thus, the trough and ridge axes of the intermediate waves tilt back with height in the lower part of the domain. The most rapid shift of phase (the strongest tilt with height) occurs near the low-level relative minimum in the amplitude. The height of the region of strongest tilt seems to be inversely correlated with the growth rate. When the rapid phase shift occurs at the lowest levels the growth rates are largest. When the phase shift occurs mainly at higher levels the growth rate is less. This result is consistent with the energetics.

The available potential energy conversion is the primary source of energy for these waves. This energy conversion from the mean flow to the eddy is shown in Figs. 6–8. It depends upon the wave amplitude and vertical derivative, the mean density and the vertical shear of the basic wind. The vertical derivative of the wave eigenvector will be partly proportional to the strength of the phase tilt and partly proportional to the amplitude. The other three quantities decrease as the level of greatest tilt becomes higher. It follows that the maximum baroclinic energy conversion is also less, thus corroborating the smaller growth rates. (The volume-integrated energy conversion must be normalized by the volume-integrated eddy energy in order to precisely compare it with the growth rates.) In the Eady–Green problem, the mean density and vertical shear are independent of height and the structure of the wave dictates the vertical structure of baroclinic energy conversion.

The changes in the complex phase frequency as γ is varied exhibit a dramatic influence by the interior potential vorticity gradient $\bar{Q}$. One can also express the forcing by the z boundary conditions as a delta function in the potential vorticity gradient (Bretherton, 1966). The forcing by the boundaries will depend upon the amplitude of the wave as does the interior forcing. For the Eady–Green problem the forcing by the boundaries will be different for different γ. For the Narrow tropopause model the upper boundary forcing is immaterial due to the exponential decay with height of ϕ and mean density. The lower boundary is made independent of γ by the ϕ normalization, since the mean velocity field is unaltered by γ. Thus the analysis reduces to an examination of the projection of $\bar{Q}$ onto $|\phi|^2$. Recall that the most rapidly amplifying intermediate and short waves are those where $\bar{Q}$ is most positive. The slowest growing waves occur when the β terms in $\bar{Q}$ are most negative. The phase speed is slowest where $\bar{Q}$ is largest and conversely. This result agrees intuitively with the stability and propagation bounds derived by Pedlosky (1964, see his eqs. 4.1.18 and 4.1.9). An analogous bound upon the phase speed, C_r, for the Eady–Green waves would be

$$\frac{-\beta(\sin\gamma - r\cos\gamma)}{2\alpha^2} \le C_r \le 1$$

The minimum allowable phase speed is decreased as the β terms become larger. In the Eady–Green problem, the propagation speed is also a maximum for the smallest $\bar{Q}$ and a minimum when $\bar{Q}$ is largest. However, the growth rate spectra for these two extremes in $\bar{Q}$ are identical in the Eady–Green problem.

This Eady–Green result can be partially elucidated by the structure that these waves adopt. The low rigid lid makes the upper boundary condition a significant factor in the stability analysis. The necessary conditions derived by Pedlosky (1964) or Blumen (1968) involve not only properties of the mean flow, but also the eddy amplitude and, for the former, the complex phase speed. A similar condition can be derived for this problem:

$$\mathrm{Im}(\omega)\left\{\int_{-l}^{l}\int_{0}^{1}\frac{|\phi|^2\bar{Q}}{|U-c|^2}\,dz\,dy + \int_{-}^{l}\frac{|\phi|^2}{|1-c|^2}\bigg|_{z=1}\frac{-|\phi|^2}{|c|^2}\bigg|_{z=0}dy\right\}=0 \qquad (5)$$

where c is the complex phase speed in the along-flow direction and $l = \pi/m$. Implicit in (5) are $\varepsilon = 1$, $U = z$ and an incompressible fluid. In the Eady–Green problem $\bar{Q}$ has opposite sign at the two extremes $\gamma = 90$ and $\gamma = 270$ (when $m = 0$). The vertical structure and propagation speed are quite different at these two angles, but the growth rate is not. The result is that the boundary terms have the same magnitude but opposite sign for $\gamma = 90$ and $\gamma = 270$. The first integral in (5) is also unchanged in magnitude, but opposite in sign leaving the bracket term in (5) still zero.

The Eady–Green and Narrow tropopause cases are somewhat complicated to analyze because the boundary and interior forcing effects intermingle. In the Eady–Green problem, both vertical boundary conditions are important. The boundary conditions (4) generally change with γ. But the amplitude normalization makes the lower boundary term in expressions such as (5) independent of γ.

And allowing for compressibility, limiting the mean flow vertical shear and placing the upper lid at a high altitude makes the upper boundary forcing insignificant in the Narrow tropopause case. The Eady–Green model can be so modified, making the upper boundary forcing negligible. Fig. 10 shows growth rate and phase speed spectra for the case where $U = z$, $\Omega = -0.5$, $\varepsilon = 1$ and the upper lid is at $z = 5$. Now that the influence of the upper boundary has been removed, the growth rate spectrum is much more comparable to that found for the Narrow tropopause case. The growth rates are largest when the β terms are largest and positive. Essentially, there is stability when $\bar{Q}$ is negative. This result is understandable if the boundary forcing is redefined as a delta-function potential vorticity gradient (Bretherton, 1966, p. 330) and is assimilated into $\bar{Q}$. A necessary condition is simply that the new $\bar{Q}$ change sign somewhere in the domain. The delta function at the lower boundary has negative sign. Hence, instability is possible only when the interior potential vorticity gradient is positive, as long as the upper boundary forcing can be neglected. The Narrow case results are now more perspicuous for analogous reasons. Once again the delta function $\bar{Q}$ at the bottom boundary is of negative sign. Instability is possible as long as the interior $\bar{Q}$ has a positive value somewhere. As the β terms become smaller (more negative) the range and values of positive $\bar{Q}$ diminish as do the growth rates. The growth rates are largest where the β terms are largest since the values of the interior $\bar{Q}$ are also positive and greatest. The bottom boundary forcing can be removed by replacing the lower boundary condition with $\phi_z = 0$. In the Narrow tropopause case, instability is now possible only when the interior $\bar{Q}$ changes sign; for $m = 0$ the most unstable waves occur where the β terms are most negative (curve B in Fig. 9). In the Eady–Green problem all waves are stabilized since $\bar{Q}$ is constant.

The primary problem of interest here is the Narrow tropopause case. This problem allows compressibility, which, when coupled with the placement of the upper rigid lid at a high altitude, makes that boundary's influence upon the solution slight. The influence of the lower boundary can be projected into the interior forcing by an appropriate normalization. $\bar{Q}$ is not uniform, instead, it has important vertical structure. These complexities probably force both parts of the complex phase frequency and eigenvector structure to change with γ for less idealized fluids than that described by the Eady–Green formulation.

4. Channel solutions

In this section some solutions of (3a) are analyzed for a channel domain that is oriented along the mean flow. The method of solution is

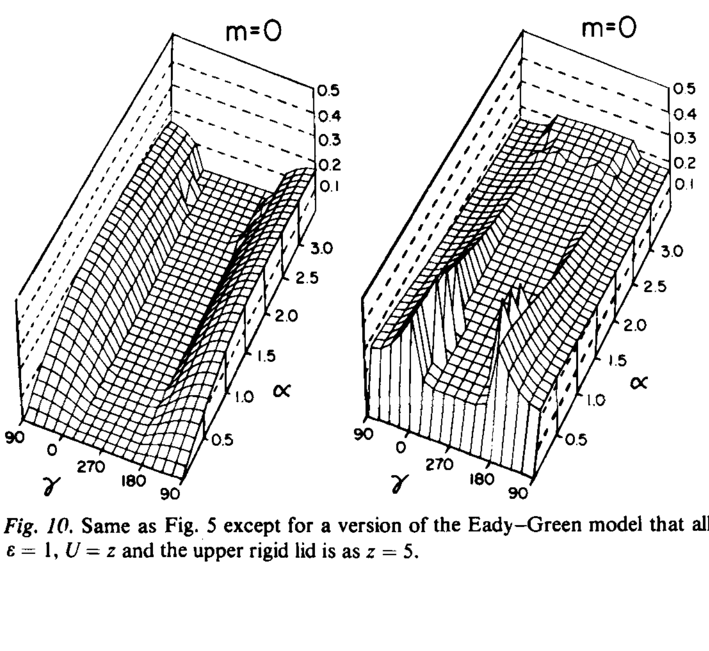

Fig. 10. Same as Fig. 5 except for a version of the Eady–Green model that allows compressibility, where $\Omega = -0.5$, $\varepsilon = 1$, $U = z$ and the upper rigid lid is as $z = 5$.

described at the end of Section 2. The asymptotic series solutions sought for ϕ and ω are truncated after two terms. Therefore, these results only show the qualitative features of the channel solutions. It is reasonable to discuss this approximate solution given the nature of the assumptions inherent to this type of study. The complex phase frequency spectra are the same as those for the $m = 0$ plane waves to second order in the expansion parameter. The channel solutions have finite horizontal width unlike the plane waves described in the previous section.

Channel cross sections of the wave amplitude and phase as well as the mean baroclinic energy conversions are plotted in Fig. 11 for $\gamma = 135$ and $\alpha = 2.0$. The viewing angle for these cross sections is upstream; the mean flow is directed out of the page. The channel width is π/k, meaning that the x and y wavelengths are essentially equal. The amplitude has two relative maxima as was found for the plane waves. The lowest-order amplitude is symmetric in y with maximum value at $y = 0$. The second-order forcing function involves the y derivative of the lowest-order solution so it is asymmetric in y. As is evident in Fig. 11, the amplitude is enhanced for $y < 0$ and diminished for $y > 0$ by the second term in the ϕ series. At second order, the forcing function and solution are both zero at $y = 0$. Therefore, the amplitude and phase structures of the eddy at $y = 0$ are equivalent to that found for the corresponding $m = 0$ plane wave. This can be verified by inspection of Fig. 6. The height of the upper level relative maximum has been slightly lowered as well. The phase angles for this wave show both vertical and cross-flow variation. The increasingly negative phase angles with height indicate that the trough and ridge axes of the wave tilt back upstream with height in the lower portion of the domain. Also, in the lower part of the domain, the phase angles increase with y indicating horizontal tilts from west to east for $\gamma = 135$. This tilt makes the solution look similar to the $m = k$ plane wave at low levels. Above $z = 0.4$, the horizontal tilt reverses and the wave axes are tilted more from south to north. Consistent with the amplitude structure, the baroclinic energy conversion is also increased for $y < 0$ and decreased for $y > 0$. It is largest at the bottom surface. The horizontal phase tilts do not induce barotropic energy conversion because the mean flow has no cross-channel variation. However, they do imply

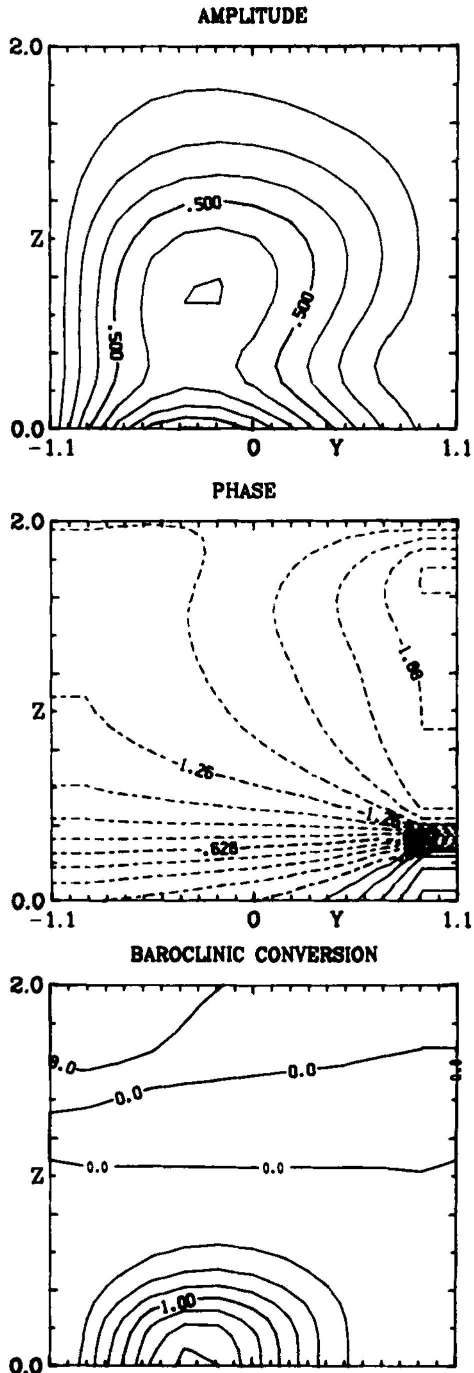

Fig. 11. Channel cross-sections of eddy pressure amplitude and phase and baroclinic energy conversion, for the Narrow tropopause case with $\alpha = 2.0$ The contour intervals are 0.125, 0.05π and 0.25 respectively.

transport and convergence of horizontal eddy momentum. There is transport of momentum from the left to the right side of the channel at low levels and much weaker transport the opposite direction at high levels. Integrated over the volume of the domain, the net momentum convergence is zero. The eddy momentum convergence occurs mainly at low levels where the eddy amplitude is enhanced. Divergence occurs at low levels where the eddy amplitude is diminished. Thus at low levels, the mean flow is accelerated where the eddy amplitude is decreased and decelerated where the amplitude is increased.

The short wave solutions display similar asymmetry in y. As for the plane waves, the channel short waves are strongly bottom trapped with weaker vertical tilts. The horizontal tilts of these waves are also weaker as is visible in Fig. 12.

There is left–right symmetry in the solutions for orientation angles greater or less than $\gamma = 90$. That is, these cross sections display solutions for $\gamma = 135$, yet the solutions for $\gamma = 45$ are the same except left and right are reversed. In other words, for $\gamma = 45$ the amplitude and energy conversion are enhanced for $y > 0$ and so forth.

5. Compendium

This study has sought to expatiate the effects of variable orientation of a mean flow, which only varies with height, upon the properties of unstable waves imbedded in that flow. Most previous stability analyses were restricted to zonal flows; most geophysical fluids are not. Only the linearly variable Coriolis (β) terms were changed by different orientations in this model. The properties of a prescribed fluid identified as the Narrow tropopause case (Grotjahn, 1980) were focussed upon. In addition, an incompressible fluid with constant linear shear, referred to as the Eady–Green case, was also examined because of its simplicity. Plane wave solutions and solutions for a channel domain were analyzed. Intermediate and short wavelength solutions were emphasized.

The stability and propagation speed of the wave is greatly changed for different orientation angles γ of the mean flow. The vertical structure of the modes is also altered by the choice of γ. Changing the orientation of the plane waves relative to the mean flow significantly modifies their properties.

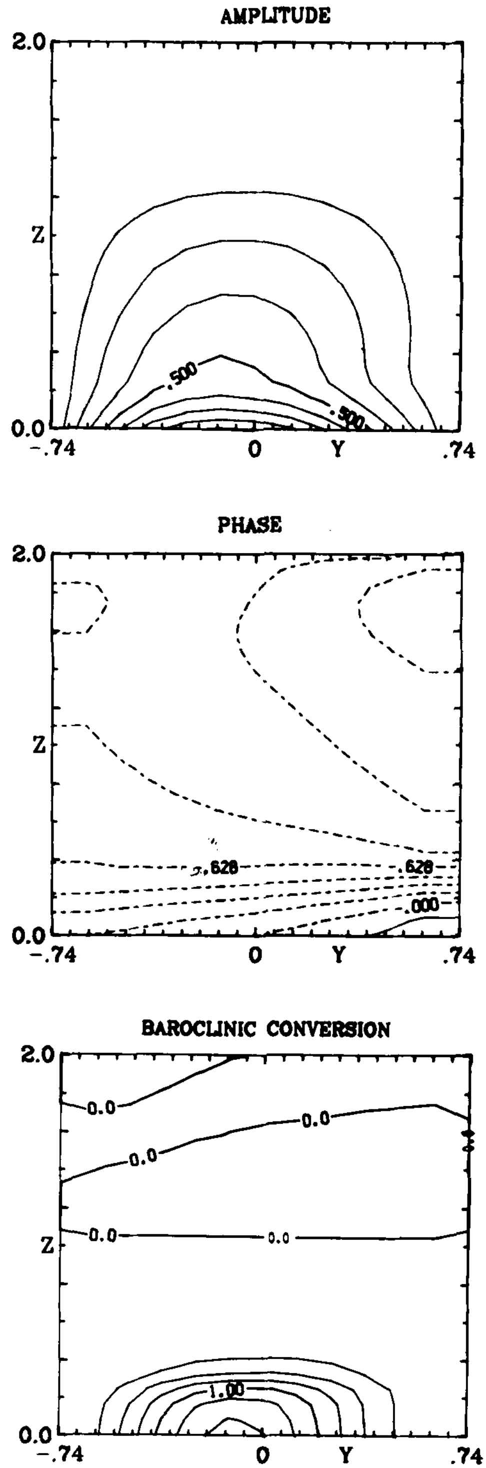

Fig. 12. Same as Fig. 11 except for $\alpha = 3.0$.

The side walls, in the channel model, have large effects upon the horizontal structure of the modes. It was found that the wave properties could be related to the distribution and magnitude of the total interior potential vorticity gradient, $\bar{Q}$.

More specifically, the instability of the plane waves was greatest when $\bar{Q}$ was greatest; that is, where the β terms were largest. The slowest growing waves occurred for angles γ where the β terms were most negative (smallest). When the two β terms cancelled, some of the long wavelengths had large growth rates; otherwise, the long waves were nearly neutral. In general, westerly-type flows were more unstable than easterly-type flows. The phase speed varied with γ in reciprocal fashion to the growth rate. The fastest moving waves were those imbedded in easterly flows where $\bar{Q}$ was smallest. The slowest waves were embedded in westerly flows where $\bar{Q}$ was largest. A component of the phase speed was generally directed down the mean current. For $m = 0$, the waves propagate in the precise direction of the mean flow. Assuming that the β terms in this problem affect the phase speed in a manner similar to the well-known retrogression of barotropic Rossby waves in a uniform westerly flow, then this result seems quite reasonable. The vertical structure was delineated in terms of the eigenvector amplitude and phase. The amplitude profiles for the intermediate waves typically had two relative maxima, one near $z = 0.8$ and one at the bottom surface. The bottom surface amplitude was fixed by a normalization. The upper maximum was greatest when $\bar{Q}$ was largest and vice versa. The position of the upper amplitude maximum seemed to be tied to the height of the largest value in the $\bar{Q}$ profile. The low-level relative minimum in amplitude was highest in elevation and least in amplitude for the smallest $\bar{Q}$ and conversely for the largest $\bar{Q}$. The plane wave trough and ridge axes tilted back upstream with height. This phase shift with height was most rapid at the low-level minimum in the amplitude profile. This result is consistent with the smaller growth rates for smaller $\bar{Q}$ since potential energy conversion is increasingly inhibited at higher altitudes by the exponential decay of mean density and eddy amplitude. Similar changes with γ were found for the short waves. However, the alterations are less visible because these waves are strongly bottom trapped. The Eady–Green formulation reproduced most, but not all, of these conclusions; the differences mainly arise from the low upper rigid lid and consideration of incompressible fluid. It seems reasonable to infer that these conclusions epitomize effects anticipated for less idealized fluids than that described by the Eady–Green model.

Some general conclusions were drawn from approximate calculations of the channel solutions. The phase speed and growth rate spectra for the channel modes are equivalent, to second order in the asymptotic series, with the corresponding $m = 0$ plane waves. The structure of the channel modes is asymmetric in the cross-channel direction, y. The amplitude and baroclinic energy conversion are enhanced on one side of the channel and diminished on the other side. Which side is enhanced depends upon the value of γ relative to 90. For south-westerly flow ($\gamma = 45$), the amplitude is increased on the right, or north side of the channel. For northwesterly flow ($\gamma = 135$), the amplitude is increased on the south side of the channel as shown in Figs. 11 and 12. To second order, the channel mode structure at $y = 0$ is identical with the structure of the corresponding $m = 0$ plane wave. These modes also tilt back upstream with height and the sharpest tilts are in the lower part of the domain. In addition, these waves have horizontal tilts. For example, when $\gamma = 135$ and the channel width is π/k, the axes tilt roughly from west to east at low levels and approximately from south to north for $z > 0.4$. These horizontal tilts imply horizontal transport and convergence of eddy momentum. The mean flow is accelerated where there is divergence and decelerated where there is convergence of eddy momentum. The divergence is principally located at low levels where the amplitude was diminished. The convergence mainly happens at low levels where the amplitude was increased.

6. Acknowledgements

I wish to thank Drs C. E. Leith, W. Blumen, J. Tribbia and R. Dickinson for their comments regarding this research.

7. Appendix

SYMBOLS LIST

C complex phase speed, x component
D vertical length scale [$= 10$ km]

f_0 mean Coriolis parameter
g acceleration of gravity
k x wavenumber
L Rossby radius of deformation at surface: Horizontal length scale [≈ 1100 km]
m y wavenumber
$\bar{Q}$ total interior potential vorticity gradient [$= \bar{q}_y - r\beta \cos \gamma$]
q eddy potential vorticity
$\bar{q}_y$ cross-flow interior potential vorticity gradient
r aspect ratio [$m = rk$]
x along-flow coordinate
y cross-flow coordinate
z vertical coordinate
α [$=(k^2 + m^2)^{1/2}$]
β first meridional derivative of f
γ orientation angle clockwise from northward
ε [$=f_0^2 L^2/g\kappa D$]
θ_s horizontal mean potential temperature
κ static stability [$= D(\ln \theta_s)_z$]
ρ_s horizontal mean density profile
ϕ eddy pressure
Ω [$=(\ln \rho_s)_z$]
ω plane wave phase frequency

REFERENCES

Blumen, W. 1968. On the stability of quasi-geostrophic flow. *J. Atmos. Sci. 25*, 929–931.

Bretherton, F. P. 1966. Critical layer instabiity in baroclinic flows. *Quart. J. Roy. Meteor. Soc. 92*, 325–334.

Brode, R. W. and Mak, M. 1978. On the mechanism of the monsoonal mid-tropospheric cyclone formation. *J. Atmos. Sci. 35*, 1473–1484.

Eady, E. T. 1949. Long waves and cyclone waves. *Tellus 1*, 33–52.

Frederiksen, J. S. 1979. Baroclinic instability of zonal flows and planetary waves in multi-level models on a sphere. *J. Atmos. Sci. 36*, 2320–2335.

Green, J. S. A. 1960. A problem in baroclinic stability. *Quart. J. Roy. Meteor. Soc. 86*, 237–251.

Grotjahn, R. 1979. Cyclone development along weak thermal fronts. *J. Atmos. Sci. 36*, 2049–2074.

Grotjahn, R. 1980. Linearized tropopause dynamics and cyclone development. *J. Atmos. Sci.* in press.

Killworth, P. D. 1979. On the propagation of stable baroclinic Rossby waves through a mean shear flow. *Deep Sea Res. 26*, 997–1031.

McIntyre, M. E. 1970. On the nonseparable baroclinic parallel flow instability problem. *J. Fluid Mech. 40*, 273–306.

Miles, J. W. 1964. Baroclinic instabiilty of the zonal wind. *Rev. Geophys. Space Phys. 2*, 155–176.

Niehaus, M. C. W. 1980. Instability of non-zonal baroclinic flows. *J. Atmos. Sci. 37*, 1447–1463.

Pedlosky, J. 1964. The stability of currents in the atmosphere and ocean: Part 1. *J. Atmos. Sci. 21*, 201–219.

Pedlosky, J. 1979. *Geophysical fluid dynamics*. New York: Springer-Verlag Publ. Comp. 497–504.

Robinson, A. R. and McWilliams, J. C. 1974. The baroclinic instability of the open ocean. *J. Phys. Oceanogr. 4*, 281–294.

СВОЙСТВА УОТОЙЧИВОСТИ ПРОИЗВОЛЬНО ОРИЕНТИРОВАННОГО СРЕДНЕГО ТЕЧЕНИЯ

Анализируются линейные свойства возмущений, растущих в среднем течение, ориентированном в горизонтальном направлении. Зональное течение изменяется только с высотой. Скорость роста, фазовая скорость и структура волн драматически изменяются с ориентацией среднего течения и волн. Эти свойства связаны с вертикальным профилем среднего градиента потенциального вихря $\bar{Q}$. $\bar{Q}$ достигает наибольшего значения для тех направлений, для которых Кориолисовы члены наиболее положительны, и наименьшего значения для тех направлений, отрицательны. Когда значение $\bar{Q}$ максимально, скорости роста наибольшие, скорость распространения наименьшая, амплитуды возмущений на верхнем уровне наибольшие, а на нижних уровнях наиболее резко проявляется вертикальный наклон ложбин и гребней. Противоположные свойства наблюдаются, когда значение $\bar{Q}$ минимально. Ограничение горизонтальных размеров волны (введением боковых границ) вызывают поперечную к потоку асимметрию в структуре волны и приводит к горизонтальному наклону волновых осей.